CrystEngComm

Accepted Manuscript

ROYAL SOCIETY OF CHEMISTRY

www.rsc.org/crystengcomm

Roles of Temperature, Solvent, M/L ratios and Anion in Preparing the Complexes Containing Himta Ligand

Tiantian Yu,[a] Shimin Wang,[b] Xuemin Li,[a] Xiaoli Gao,[a] Chunlin Zhou,[a] Jiajia Cheng, Baojun Li,[a] Jinpeng Li*,[a] Junbiao Chang,[a] Hongwei Hou,[a] Zhongyi Liu*[a]

ABSTRACT: In order to systematically investigate the influence of factors on the structures of coordination complexes, $\{[Cu(imta)_2]\cdot 2.5H_2O\}_n$ **(1)**, $[M(imta)_2]_n$ M=(Co, Mn, Cd) **(2~4)**; $[Pb(imta)_2]_n$ **(5)**; $[M(imta)_2(H_2O)_4]\cdot 2H_2O$] M=(Co, Mn, Ni, Zn) **(6~9)** {H-imta=2-[4-(1H-imidazole-1-ylmethyl)-1H-1,2,3-triazol-1-yl] acetic acid}, have been prepared and characterized by single-crystal X-ray diffraction analyses. **1** is a 2-D MOF with one-dimensional open channels, **2**, **3** and **4** are isostructural and display (3,6)-connected 3D frameworks which can be simplified into novel Schläfli symbols of $(4\cdot 6^2)_2(4^2\cdot 6^{10}\cdot 8^3)$. **5** features a (3,6)-connected topology with the Schläfli symbol $(4^2\cdot 6)_2(4^4\cdot 6^2\cdot 8^9)$. **6~9** are isostructural and mononuclear, which are further stretched to a 3D supramolecular structure through hydrogen bonding. Based on complexes **2** (or **3**) and **6** (or **7**), a systematic and comprehensive investigation of temperature, solvent, M/L ratios and anion on complex architectures were carried out. The present results may help unravel the mechanism for the roles that synthesis parameters play in the formation of complex structures, and provide insight into the discovery of new interesting compounds. In addition, the photoluminescent properties of **2~9** were also studied.

Introduction

* To whom correspondence should be addressed. E-mail: ljp-zd@163.com

[a]*College of Chemistry and Molecular Engineering, Zhengzhou University, Zhengzhou 450001, Henan, P. R. China*

[b]*College of Material and Chemistry Engineering, Henan Institute of Engineering, Zhengzhou, 451191, P. R. China*

Electronic supplementary information (ESI) available: The X-ray crystallographic files in CIF format. CCDC reference numbers 1437785-1437793 are for **1~9**, respectively.

The rational design and preparation of metal-organic complexes is currently attracting significant attention in the field of crystal engineering and supramolecular chemistry not only for their interesting structures but also for special functional material purpose.[1-3] So far, tremendous efforts have been devoted to synthesizing metal-organic coordination complexes with interesting topologies and properties.[4] Up to date, it is still challenging to control effectively complex architectures. Control in constructing complexes with well-defined structures and useful functions still remains a distant prospect in crystal engineering owing to the influence of many factors, such as solvent system, metal-ligand ratio, temperature and anion.[5-8] In the past few decades, studies in this field have been focused on the elucidation of the role of these foregoing factors. In fact, temperature can affect the behavior of crystalline systems which has been widely reported,[9] For example, Cheng and co-workers obtained $\{[Cu^{II}(btz)]\cdot 0.5H_2O\}_n$ and $[Cu^{II}Cu^{I}_2(btz)_2]_n$ [H_2btz =1,5-bis(5-tetrazolo)-3-oxapentane)] with different chiralities from the same starting materials through altering different temperature.[9a] Furthermore, controlling the solvent system can also significantly affect structure of the complex,[10] 2-D sheet $\{(Me_2NH_2)\cdot[Zn(tci)]\cdot 0.5DMF\}_n$ and 3-D framework $\{(Me_2NH_2)\cdot[Zn(tci)]\cdot 2DMF\}_n$ (Me_2NH_2=protonated dimethylamine, H_3tci=tris(2-carboxyethyl)isocyanuric acid) were reported by Sun group by simply change solvent systems from DMF-EtOH-H_2O (5 mL/2 mL/1 mL) to DMF-EtOH (5 mL/2 mL).[10a] Besides, metal ligand ratio also play important role in the formation of the structure,[11] such as, Wang and his co-researchers changed the molar ratio of the reactant metal salt and ligands from 1:1:1 to 1:1:3, resulting in three entangled coordination polymers.[11a] However, to the best of our knowledge, many of complexes were synthesized by altering simple variables such as temperature, solvent composition, anion, etc. The comprehensive effect of various influence factors on the formation of coordination complexes is less well understood and systematic studies are still rare.[12,13] From the viewpoint of crystal engineering, a detailed understanding of the role that these variables play in complex synthesis remains one of the most important advancements in the field. This promotes us to carry out systematic and comprehensive investigation of various influence

factors on complex architectures.

On the basis of the above considerations, we design and synthesize a new 2-[4-(1H-imidazole-1-ylmethyl)-1H-1,2,3-triazol-1-yl] acetic acid ligand. Nine new complexes were further obtained under hydrothermal conditions, which display various topological structures. The existence of easily obtained crystal structures of **2**, **3**, **6** and **7** offers an opportunity to examine the role of various reaction variables in determining specific structure forms. Herein, the effect of various reaction variables on building the architectures of complexes was investigated in details. In addition, the fluorescence properties of complexes **2-9** were also investigated.

Experimental section

Materials and general methods.

All materials were of analytical grade and obtained from commercial sources without further purification. Infrared spectra data were recorded on a BRUKER TENSOR 27 spectrophotometer with KBr pellets in the 400-4000cm^{-1} region. Elemental analyses (C, H and N) were carried out on a FLASH EA 1112 elemental analyzer. The luminescent measurements for the solid samples were performed at room temperature using a HITACHI F-4600 fluorescence spectrophotometer.

Preparation of the Himta Ligand. Ligand Himta was synthesized according to the procedure described in Scheme 1. (i) The synthetic route of *1-(prop-2-yn-1-yl)-1H-imidazole*: 1-(prop-2-yn-1-yl)-1H-imidazole was according to the literature.[14]

(ii) *Synthesis of 2-[4-(1H-imidazole-1-ylmethyl)-1H-1,2,3-triazol-1-yl] acetic ether*: The 1-(prop-2-yn-1-yl)-1H-imidazole (3.83g, 0.036mol) were dissolved in 50 mL of tert-butyl alcohol and water (1:1) mixed solution, ethyl 2-azidoacetate (5.12g, 0.040mol), $CuSO_4 \cdot 5H_2O$ (0.899g, 0.004mol) and sodium isoascorbate (1.43g, 0.007mol) were added sequentially, followed ultrasonic treatment for 3h. Ammonia (10 mL) and NH_4Cl (10 mL) solution were added. The mixture was extracted with H_2O/CH_2Cl_2. The organic layer was dried over Na_2SO_4 and concentrated to give

yellowish-white solid. The crude product was crystallized from ethyl acetate as light faint yellow powder (5.41g, 0.023mol) in 63% yield.

(iii) *Synthesis of Himta*: The above-mentioned ester (5.41g, 0.023mol) was dissolved in 15 mL of CH_3OH and H_2O (1:1) mixed solutions, NaOH (1.12g, 0.028mol) was added. The mixture was stirred at room temperature for 24h. The precipitated product was filtered, and then dissolved in 15 mL of H_2O. Then the aqueous solution was acidied to pH 7.0 by HCl solution. After removing the solvent H_2O by reduced pressure distillation, the *Himta* (3.52g, 0.017mol) was obtained in 47% yield. Mp: 240-243°C. ^{1}HNMR (400 MHz, DMSO): 8.337(s,1H), 7.930 (s,1H), 7.288-7.172 (d, 2H), 5.356 (s, 2H), 4.906 (s, 2H). IR spectra (KBr, cm^{-1}): 3425s, 3142m, 3007m, 2436w, 2079w, 1619s, 1545w, 1515m, 1427s, 1401s, 1325s, 1325s, 1280m, 1227s, 889m, 836s, 814s, 730s, 684s, 586s, 519s.

Preparation of $\{[Cu(imta)_2]\cdot 2.5H_2O\}_n$ (1)

A mixture of Himta (8.3 mg, 0.04 mmol) and $CuSO_4\cdot 5H_2O$ (5.0 mg, 0.02 mmol) in solvent of H_2O/CH_3OH (1:1, 4 mL) were placed in a 25 ml Teflon-lined stainless steel container, heated to 90°C for 3 days, and then cooled to room temperature, blue crystals of **1** were collected (yield: 30% based on copper). Anal. Calcd for $C_{32}H_{42}Cu_2N_{20}O_{13}$: C, 36.88; H, 4.07; N, 26.89. Found: C, 36.76; H, 4.18; N, 26.56%. IR spectra (KBr/pellet, cm^{-1}): 3426m, 3142m, 1636s, 1523m, 1388s, 1297m, 1092m, 950w, 816m, 726m, 700w, 653m, 618w, 518w.

Preparation of $[Co(imta)_2]_n$ (2)

Polymer **2** was synthesized hydrothermally in a Teflon-lined stainless steel container by heating a mixture of Himta (8.3 mg, 0.04 mmol) and $CoCl_2\cdot 6H_2O$ (4.8 mg, 0.02 mmol) in 3 mL of H_2O/CH_3OH (1:2) mixed solvent at 100°C for 3 days, and then cooled to room temperature, pink crystals of **2** were collected. (yield: 69% based on cobalt). Anal. Calcd for $C_{16}H_{16}CoN_{10}O_4$: C, 40.77; H, 3.43; N, 29.72. Found: C, 40.67; H, 3.32; N, 29.79%. IR spectra (KBr/pellet, cm^{-1}): 3417m, 3002m, 1610s, 1514s, 1467m, 1392s, 1276s, 1186w, 1111s, 1031m, 964w, 930m, 814m, 763w, 726s, 620m,

587w, 420w.

Preparation of $[Mn(imta)_2]_n$ (3)

A mixture of Himta (8.3 mg, 0.04 mmol), and $MnSO_4 \cdot H_2O$ (3.4 mg, 0.02 mmol) in solvent of 4 mL H_2O/CH_3OH (1:3,volume ratio) were sealed in a 25 mL poly(tetrafluoroethylene)-lined stainless steel container and then heated at 160°C for 3 days and finally cooled to room temperature, colorless transparent stripe crystals of **3** were collected. Yield: 60% based on manganese. Anal. Calcd for $C_{16}H_{16}MnN_{10}O_4$: C, 41.12; H, 3.46; N, 29.98. Found: C, 41.05; H, 3.23; N, 29.67%. IR spectra (KBr/pellet, cm^{-1}): 3439m, 3002m, 1611s, 1514m, 1423m, 1391s, 1276m, 1186w, 1109m, 965w, 843m, 724m, 620m, 585w, 414w.

Preparation of $[Cd(imta)_2]_n$ (4)

Polymer **4** was synthesized from a mixture of Himta (8.3 mg, 0.04 mmol), $Cd(NO_3)_2 \cdot 4H_2O$ (6 mg, 0.02 mmol) and H_2O (3 mL), which was sealed in a Teflon-lined stainless steel vessel (25 mL), and heated to 150°C for 72 h, followed by cooling to room temperature at 5ºC/h. Colorless block crystals of **4** were collected. The yield of the product **4** was 55%, based on cadmium. Anal. Calcd for $C_{16}H_{16}CdN_{10}O_4$: C, 36.61; H, 3.08; N, 26.69. Found: C, 36.65; H, 3.19; N, 26.78%. IR spectra (KBr/pellet, cm^{-1}): 3440m, 3003m, 1601s, 1515m, 1469w, 1388s, 1323m, 1277m, 1108m, 1028w, 843w, 653m, 584w, 412w.

Preparation of $[Pb(imta)_2]_n$ (5)

The reaction condition was the same as that for **3**, except that $Pb(Ac)_2 \cdot 3H_2O$ (7.6 mg, 0.02 mmol) instead of $CoCl_2 \cdot 6H_2O$ (4.8 mg, 0.02 mmol), colorless block crystals of **5** suitable for single crystal X-ray diffraction were obtained (yield: 65% based on lead). Anal. Calcd for $C_{16}H_{16}N_{10}O_4Pb$: C, 31.01; H, 2.61; N, 22.61. Found: C, 31.05; H, 2.73; N, 22.57%. IR spectra (KBr/pellet, cm^{-1}): 3440m, 3080s, 2987m, 1610s, 1509s, 1465m, 1385s, 1340s, 1289s, 1232s, 1190w, 1167w, 1140m, 1060s, 920s, 858m, 779m, 722s, 684m, 642m, 583w, 438m.

Preparation of $[Co(imta)_2(H_2O)_4]\cdot 2H_2O$ (6)

Himta (8.3 mg, 0.04 mmol) and $CoCl_2\cdot 6H_2O$ (4.8 mg, 0.02 mmol) in 3 mL of distilled water was sealed in a 25 mL poly(tetrafluoroethylene)-lined stainless steel container, heated at 160ºC for 3 days, and then cooled to room temperature, pink crystals of **6** were collected (yield: 76% based on cobalt). Anal. Calcd for $C_{16}H_{28}CoN_{10}O_{10}$: C, 33.16; H, 4.88; N, 24.18. Found: C, 32.81; H, 4.75; N, 24.62%. IR spectra (KBr/pellet, cm^{-1}): 3408m, 3002m, 1607s, 1514m, 1424m, 1392s, 1276m, 1186w, 1077m, 964w, 930m, 841m, 740m, 620m, 587w, 419w.

Preparation of $[Mn(imta)_2(H_2O)_4]\cdot 2H_2O$ (7)

A mixture of Himta (8.3 mg, 0.04 mmol) and $MnCl_2\cdot 4H_2O$ (5.9 mg, 0.03 mmol) in solvent of H_2O/CH_3OH(1:2 volume ratio 6 mL) at 120°C for 3 days, and then cooled to room temperature, pink block crystals of **7** were collected (yield: 76% based on manganese). Anal.Calcd for $C_{16}H_{28}MnN_{10}O_{10}$: C, 33.39; H, 4.90; N, 24.34. Found:C, 33.49; H, 4.72; N, 25.79%. IR spectra (KBr/pellet, cm^{-1}): 3513s, 3136s, 2960m, 2369w, 1661m, 1599s, 1461m, 1393s, 1285m, 1160w, 1092m, 966w, 933m, 841m, 750s, 612m, 493m, 432m.

Preparation of $[Ni(imta)_2(H_2O)_4]\cdot 2H_2O$ (8)

Himta (8.3 mg, 0.04 mmol), $NiCl_2\cdot 6H_2O$ (4.8 mg, 0.02 mmol) and 3mL H_2O/CH_3OH (1:2 volume ratio) were mixed in a 25 mL Teflon-lined stainless steel container. The mixture was stirred for 30 min at room temperature and sealed, which was heated at 105°C for 3 days and then slowly cooled to room temperature at the rate 5°C/h. Finally green block crystals of **8** were collected (yield: 75% based on nickel). Anal. Calcd for $C_{16}H_{28}N_{10}NiO_{10}$: C, 33.18; H, 4.88; N, 24.19. Found: C, 33.19; H, 4.91; N, 24.75%. IR spectra (KBr/pellet, cm^{-1}): 3508s, 3137s, 2454w, 1596s, 1461m, 1394s, 1284m, 1158w, 1103m, 1038m, 1012w, 942w, 841s, 749s, 686s, 579m, 431m.

Preparation of $[Zn(imta)_2(H_2O)_4]\cdot 2H_2O$ (9)

The synthetic procedure was similar to that of **4**, except $Zn(NO_3)_2 \cdot 6H_2O$ (5.9 mg, 0.02 mmol) replaced $MnSO_4 \cdot H_2O$, the colorless block crystals of **9** were obtained (yield: 71% based on zinc). Anal. Calcd for $C_{16}H_{28}N_{10}O_{10}Zn$: C, 32.80; H, 4.83; N, 23.91. Found: C, 32.05; H, 4.62; N, 23.61%. IR spectra (KBr/pellet, cm^{-1}): 3514m, 3135s, 2945m, 1649s, 1561w, 1522s, 1464m, 1388s, 1290s, 1189w, 1107s, 1030m, 952m, 845w, 817m, 725m, 652m, 590w, 482m.

Crystal structure determination. The data of **1-9** were collected on a Rigaku Saturn 724 CCD diffractomer (Mo-*Kα*, λ = 0.71073 Å) at temperature of of 298 ± 1K. The empirical absorption corrections were applied to these complexes. Absorption corrections were accomplished by utilizing multiscan program. The data were gathered according to Lorentz and polarization effects. The structures were solved by direct methods and refined with a full-matrix least-squares technique based on F^2 with the SHELXL-97 crystallographic software package[15]. All non-hydrogen atoms were refined anisotropically while hydrogen atoms were generated geometrically. Table 1 and 2 shows crystallographic crystal data and structure processing parameters of **1-9.** Selected bond lengths and bond angles of **1**-**9** are listed in Table S1 and S2.

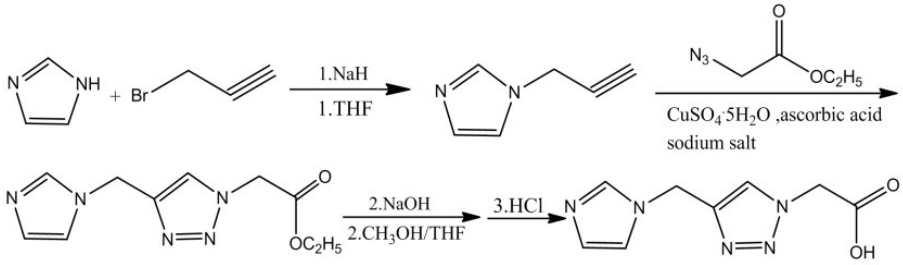

Scheme.**1**. Preparation of the Himta acetic acid ligand

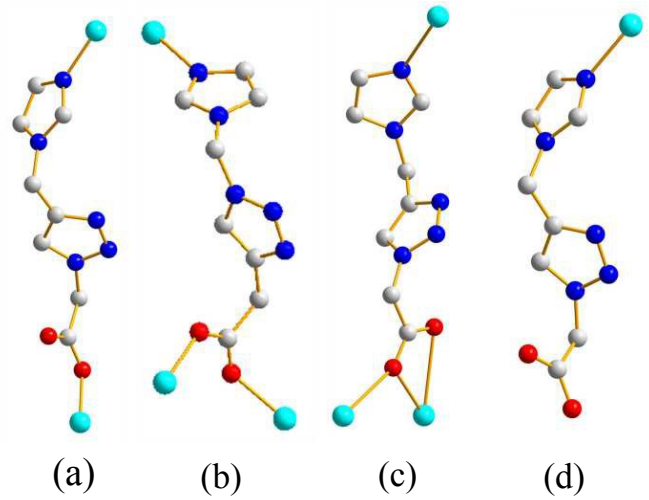

Scheme 2. Coordination modes of the Himta in complexes **1**-**9**.

Results and discussion

$\{[Cu(imta)_2]\cdot 2.5H_2O)\}_n$ (1)

Single-crystal X-ray diffraction reveals that complex **1** crystallizes in monoclinic system with space group *I2/a*. The independent unit consists of a Cu(II), two $imta^-$ ligands, two and a half lattice waters. As depicted in Figure 1a, each Cu(II) is four-coordinated by two carboxylate group oxygen atoms (O2A and O2B) and two triazole nitrogen atoms (N1 and N1C) from four different $imta^-$ ligands, and the bond lengths of Cu-N and Cu-O are 1.972(4) Å and 1.957(3) Å, respectively. The coordination geometry around Cu(II) can be described as a nearly ideal square-planar, because the O-Cu-N coordination angles range from 88.9(2)° to 91.1(2)° (Table S1). As is shown in Figure 1b, each $imta^-$ ligand adopts a bidentate bridging coordination mode, binding to two Cu(II) via imidazole-N and carboxylate-O (Scheme 2a), and each Cu(II) center is linked to four adjacent Cu centers by four bidentate ligands, furnishing a (4,4) 2D wavelike net. There is no interpenetration between adjacent layers and the 2D sheets are stacked according to the ABAB sequence along the *a*-axis (Figure 1b). As a consequence of the arrangement, a cavity-containing rhombic grid which packs along crystallographic *bc* plane and exhibits intragrid Cu···Cu separations of 12.887(3) Å and a diagonal measurement about 19.396(6) Å×16.974(3)

Å. The stacking exhibited by the grids yields microchannels that run approximately perpendicular to the layers, and the microchannels are occupied by water molecules bound together via hydrogen-bonding interactions (Figure 1c). The inter-molecular N5···O4D [2.907(8) Å], O4D···O3E [2.747(19) Å], N4···O5F [3.039(9) Å], O5F···O5G [3.136(16) Å] hydrogen bonds among the water and network are observed, which further stabilize the 3-D supramolecular network (Figure 1c and Table S3). Apart from these interactions, the 3D structure is also stabilized by π···π and CH/π stacking interactions.[16] Between two imidazole rings of two adjacent layers imta$^-$, there are π···π interactions with a centroid-to-centroid separation of 3.4549(11) Å and π···π interactions with a centroid-to-centroid separation of 4.0295(7) Å between two triazole rings of two adjacent layers imta$^-$. Additionally, between methylene and imidazole rings of imta$^-$ ligand, the C-H···π interactions at 2.698(8) Å [dihedral angle: 80.6(2)°; H/π -plane separation: 2.6266(2) Å] further stabilized the 3D structure. After the removal of the free water molecules of complex **1**, it is microporous (Figure 1d), with a total potential solvent accessible volume of 33.7% calculated using PLATON.

(a) (b)

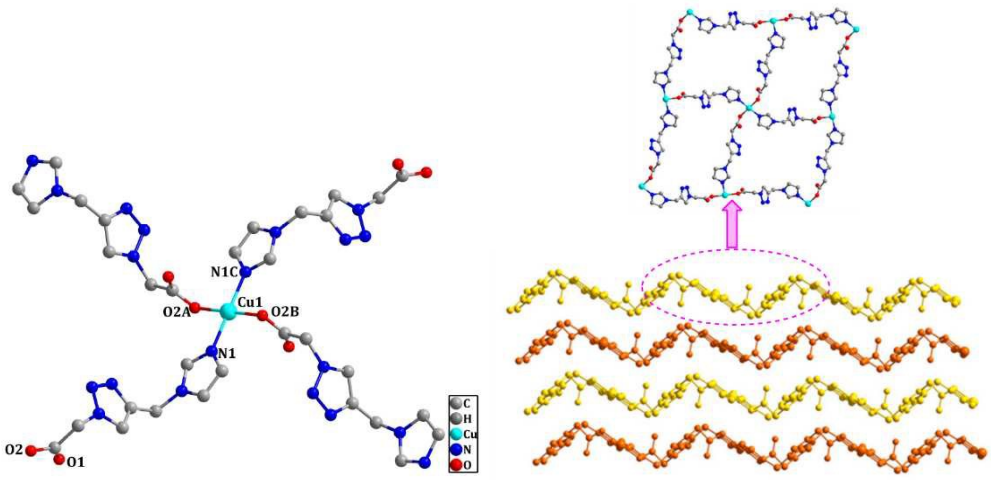

(c)

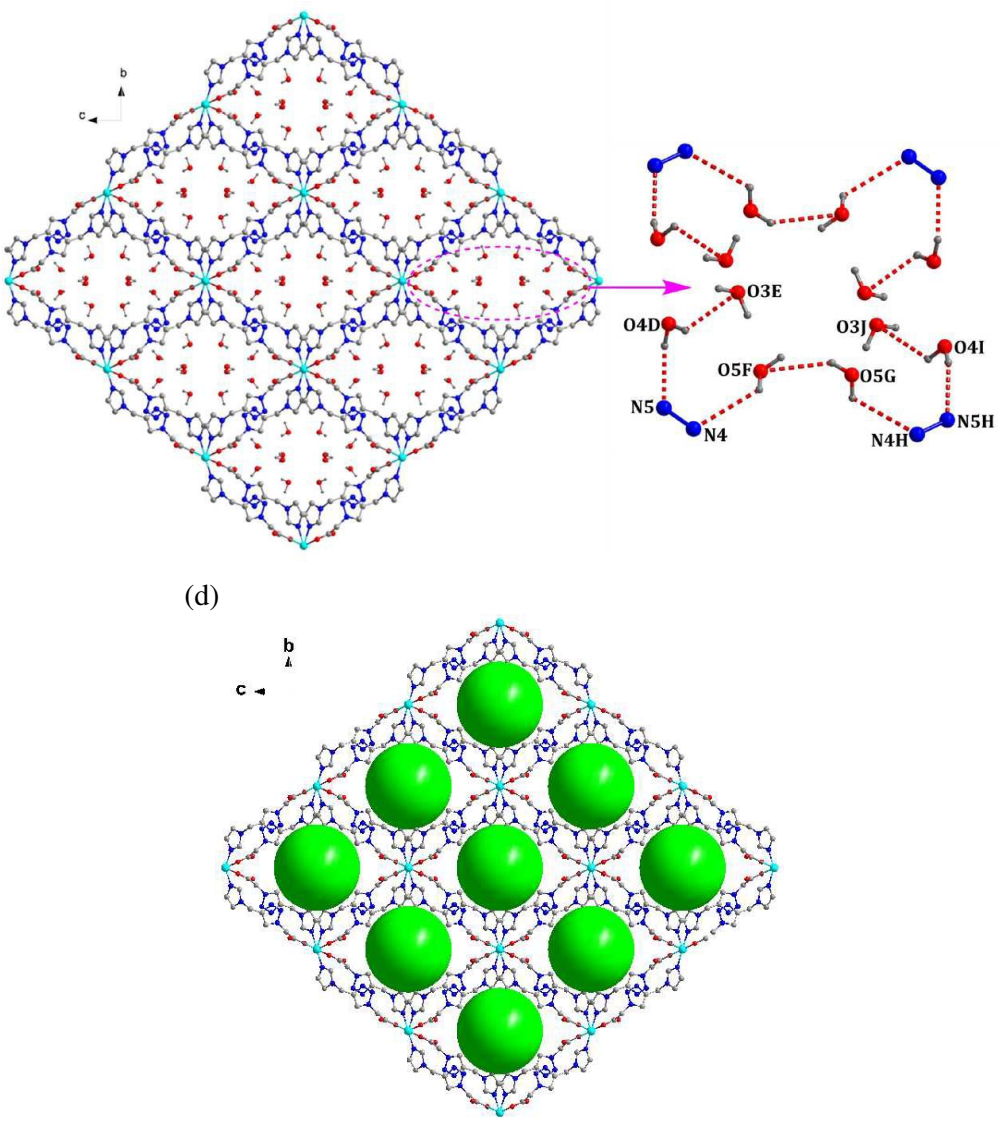

Figure 1. (a) Coordination environment of the metal atom in **1** (symmetry codes for A: 1-x, 1/2+y, 1/2-z; B: x, 1/2-y, 1/2+z; C: 1-x, 1−y, 1-z). (b) Stacking diagram of the parallel coordination sheets viewed along the *ac* plane (hydrogen atoms and free water were omitted for clarity. (c) View of the hydrogen bonds between the guest H_2O molecules and ligands (symmetry codes for D: 1-x, 1-y, 1-z; E: 1/2+x, 1-y, z; F: 1-x, -1/2+y, 1/2-z; G: -1/2+x, -1/2+y, -1/2+z; H: 1/2-x, y, -z. I: -1/2+x, 1-y, -1+z; J: -x, 1-y, -z). (d) Views of the packing diagram with large void along the *a* axis in **1**. (H_2O guest molecules removed for clarity)

$[M(imta)_2]_n$ [M = Co (2), Mn (3), Cd (4)]

Single crystal X-ray diffraction reveals that complexes **2**-**4** are isomorphous and

crystallizes in the space group $P2_1/c$. Herein, the structure of **2** will be described as representative in detail. The asymmetric unit has half of a Co atom on an inversion centre and one imta ligand in a general position. As shown in Figure 2a, the six-coordinated Co(II) ion possesses distorted octahedral coordination geometry with the equatorial positions occupied by the carboxylate oxygens and the apical ones taken up by the imidazole nitrogen atoms from the surrounding six different imta$^-$ ligands. The N-Co-O angles range from 85.64(12) to 94.36(13)°, revealing the slightly distorted octahedron with the equatorial Co-O distances of 2.080(3) and 2.131(3) Å together with Co-N of 2.173(4) Å. The coordination mode of the ligand Himta is given in scheme (b). Each imta$^-$ ligand acts as a μ_3-bridge to link three Co(II) ions through the nitrogen atom at the imidazolel moiety and the carboxylate group adopting a μ_2-η^1:η^1-bridging coordination mode. The dihedral angle between imidazolyl and triazole ring in imta$^-$ is 111.1(4)º. The carboxylate groups of imta$^-$ ligand links Co atoms into an infinite chain featuring the $Co_2C_2O_4$ 8-membered rings with the Co···Co distance of 4.843(1) Å (Figure 2b). The infinite chains are further interconnected by the apical ligation of triazole nitrogen shown as CoO_4N_2 octahedrals into a so-called rod-based[17] framework (Figure 2c, 2d). The imta$^-$ rings are almost parallel to each other resulting CoO_4N_2 octahedrals overlapped along *a* axis. It is also clear that there exist insignificant π···π stacking interactions owing to the center-to-center distances of longer than 4 Å between the layers. However, there are hydrogen bonds in complex **2** which have further stabilized the structure. The H···N distances (bond angles) of the C-H···N hydrogen bonds are 2.741(5) Å [138.6 (3)°] for C1-H1···N4, 2.723(4) Å [146.3(3)°] for C4-H4···N5. The H···O distance (bond angle) of the C-H···O hydrogen bond is 2.518(4) Å [113.7(3)°] for C4-H4···O2. To better understand the framework of **2**, topological analysis is carried out, reducing multidimensional structures to simple nodes and connection nets. Each Himta ligand connects three Co(II) ions acting as a 3-connected node, while each Co(II) ion is surrounded by six imta$^-$ ligands, which can be represented by a 6-connected node. Thus, **2** can be considered as a (3,6)-connected rtl topology with the point symbol of $\{4.6^2\}_2\{4^2.6^{10}.8^3\}$ indicated by TOPOS software[18] (Figure 2e).

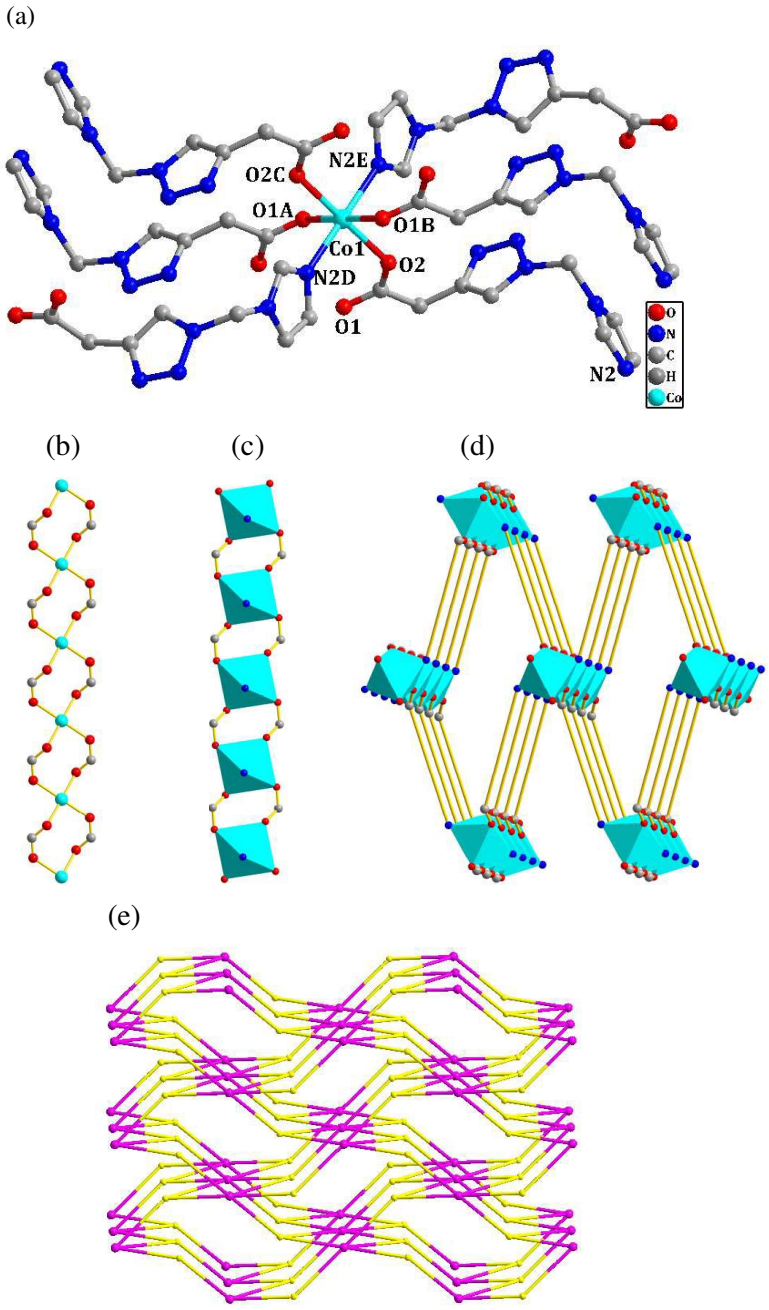

Figure 2. (a) Coordination environment of the Co(II) center in complex (symmetry codes for A: -x+2, -y, -z+1; B: x-1, y, z; C: -x+1, -y, -z+1; D: x, -y+1/2, z+1/2; E: -x+1, y-1/2, -z+1/2). (b) Chain like structure formed by the Co(II) and bridging carboxylate groups. (c) CoO_4N_2 shown as polyhedron (d) Octahedral CoO_4N_2 chains interconnected by the imta$^-$ ligands (imta$^-$ are drawn as solid lines for clarity). (e) Schematic representation of (3,6)-connected topology (color code: red ball, 6-connected Co(II) node; yellow ball, 3-connected imta$^-$ node).

$[Pb(imta)_2]_n$ (5)

Single-crystal X-ray diffraction reveals that 5 crystallizes in the orthorhombic system with *Pccn* space group. The asymmetric unit has half of a Pb atom on a two fold axis and one imta ligand in a general position. As illustrated in Figure 3a, the eight-coordinated Pb(II) ion lies on the square-antiprismatic geometry formed by six O atoms from four different $imta^-$ ligands and two N atoms from two $imta^-$ ligands. However, it should be noted that, polymer **5** show that a holodirected geometry[19] which is different from Pb(II) complexes $\{[Pb(\eta^2\text{-}OOCFcCOC_2H_4COO\text{-}\eta^2)(phen)]_2(CH_3OH)\}$ [$HOOCFcCOC_2H_4COOH$=1'-(formyl)ferrocene-1-succinic acid, phen=1,10-phenanthroline], $[Pb_6(btapca)_6]\cdot(H_2O)_2$ and $[Pb_2(btapca)_2(H_2O)_2]_n$ [H_2btapca=N,N'-bis(1,3,4-thiobiazolyl)-2,6-pyridyldicarboxamide].[20,21] The geometry of Pb(II) in **5** suggests that the lone electron pair of the metal do not stereochemically active.[22] The O-Pb-O, O-Pb-N and N-Pb-N bond angles are in the ranges of 47.91(15)-173.9(2)°, which are similar to those observed for other analogical Pb complexes.[23-25] The coordination mode of ligand Himta is given in scheme (c), different from that in **2**, each $imta^-$ ligand acts as a μ_3-bridge to link three Pb(II) ions through the imidazolel nitrogen atom and the $\mu^2\text{-}\eta^1\text{:}\eta^2$ carboxylate moiety. The dihedral angle between imidazolyl and triazole ring of $imta^-$ is 111.6(6)º, which is slightly larger than that in **2**. The carboxylate groups of imta ligand links Pb(II) into an infinite chain featuring the $Pb_2C_2O_4$ 8-membered rings. There exist two kinds of alternating chelating groups coordinated to Pb(II) ions in the infinite chains along *c* axis (Figure 3a). This connectivity pattern is repeated infinitely to create rod-like motifs and give edge shared PbN_2O_6 bisdisphenoids with the Pb···Pb separation of 4.1886(10) Å (Figure 3b). As a consequence, the rods are linked by $imta^-$, which connect each rod to four neighboring rods in the *ab* plane (Figure 3c, 3d). The PbN_2O_6 bisdisphenoids are stacked according to the ABAB sequence along the *c*-axis caused by the arrangement of the carboxyl group. Unlike **2**, there are strong π···π stacking interactions between the adjacent triazole rings with a centroid-to-centroid

separation of 3.9937(7) Å. In addition, the inter-molecular C-H···O interaction is observed in complex **5**.

According to the simplification principle, the structure of **5** is binodal with eight-connected [Pb(II) ions] and three-connected (imta$^-$ ligands) nodes and exhibits a 3D topology network. Thus, the overall structure of **5** can be described as a (3,8)-connected flu topology with the point symbol of $(4^2\cdot6)_2(4^4\cdot6^2\cdot8^9)$ calculated by the TOPOS program[18] (Figure 3e).

(a)

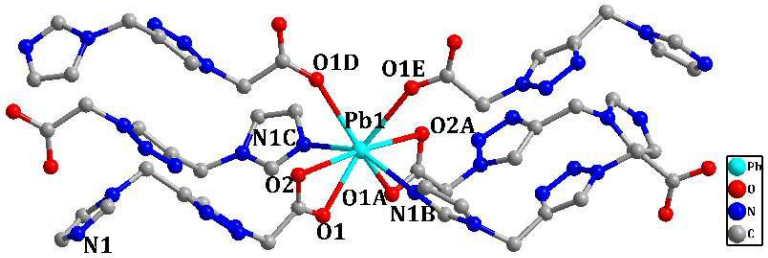

(b) (c) (d)

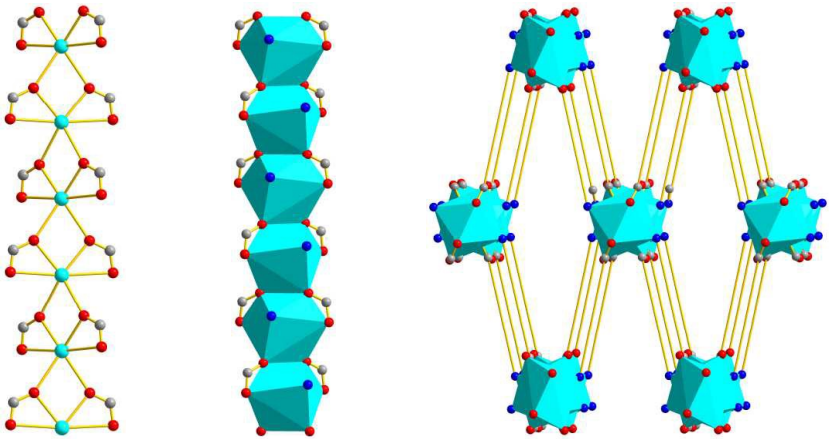

(e)

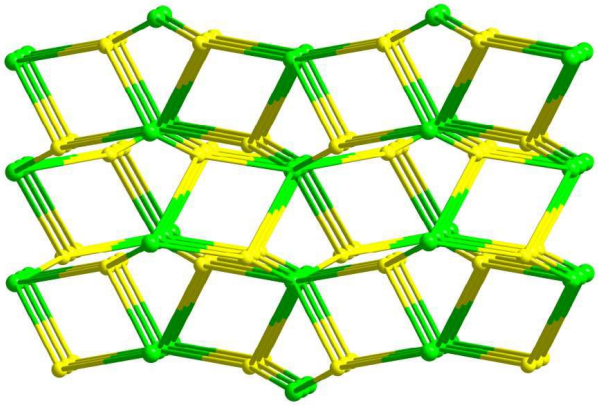

Figure 3. (a) The units structural figure of complex **5** (symmetry codes for A: -x+3/2, -y+3/2, z; B: -x+1, y-1/2, -z+3/2; C: x+1/2, -y+2, -z+3/2; D: -x+3/2, y, z+1/2; E: x, -y+3/2, z+1/2;). (b) and (c) View of the rod-like motif with edge-sharing polyhedron PbO_6N_2 along c direction. (d) View of the 3D coordination framework of **5** along the ab-plane. (e) Schematic representation of (3,6)-connected topology(color code: green ball, 6-connected Pb(II) node; yellow ball, 3-connected $imta^-$ node)

$[M(imta)_2(H_2O)_4]\cdot 2H_2O$ [M = Co (6), Mn (7), Ni (8), Zn(9)]

The X-ray diffraction analysis reveals that complexes **6-9** are isomorphous and crystallizes in the triclinic system with *P-1* space group. Herein, the structure of **6** containing Co(II) centers is selected to be discussed in detail. The asymmetric unit has half of a Co atom on an inversion centre and one coordinated imta ligand two coordinated water molecules and one lattice water in a general position (Figure 4a). The central Co1 atom is hexa-coordinated to two nitrogen atoms from two different *imta*$^-$ ligands and four oxygen atoms from four water molecules, and the coordination geometry can be described as a slightly distorted octahedral configuration. Four oxygen atoms from four water molecules consist of the equator base (the mean deviation from the plane is 0.0000Å). The bond length of Co-N is 2.146(3) Å, and the Co-O distance ranges from 2.104(3) Å to 2.129(3) Å. The bond angles around Co vary from 88.58(9)º to 180.00(12)º. The average bond lengths of Co-O and Co-N are 2.116(3) and 2.146(3) Å, which is slightly longer than the common Co-O and Co-N distances of 1.94 and 1.96 Å, respectively.[26] It is worthy to note that the imta anion acting in mono-dentate coordination mode only take part in coordination interactions with metal ions through the nitrogen atoms, which is similar to the reported of 2-(1H-benzotriazol-1-yl)acetic acid].[27]

The $[Co(imta)_2(H_2O)_4]\cdot 2H_2O$ units are connected through O-H···O hydrogen bonds involving the coordinated water molecules, lattice water and carboxyl oxygen atoms, producing a 2D supramolecular layer (Figure 4b). It deserves to be noted that two different hydrogen bonding motifs, $R_2^4(8)$ and $R_4^6(12)$, occur in the supramolecular layer (Figure 4c). The carboxyl oxygen O1 and O4 water molecules,

arranged in a square fashion with two symmetry-related molecules formed $R_2^4(8)$ hydrogen-bonding motifs. The carboxyl oxygen O1 acts as double hydrogen bond acceptor, while O4 acts as double hydrogen bond donor. The O···O distances of the hydrogen bonds are 2.764(3) Å for O4D···O1, 2.727(3) Å for O4D···O1B. Meanwhile, the carboxyl group oxygen O2 acts as double hydrogen bond acceptor, O3 water molecule acts as double hydrogen bond donor, while O9 acts as both hydrogen bond donor and acceptor, respectively, which generates a $R_4^6(12)$ ring motif and exhibits a chair conformation.[28] The O···O distances of the hydrogen bonds are 2.651(4) Å for O3G···O9, 2.740(3) Å for O3G···O2E, 2.847(4) Å for O9···O2 (Table S3). This two types of $R_2^4(8)$ and $R_4^6(12)$ rings in **6** are alternatively linked through O-H···O hydrogen bonds giving rise to a layered network that grows in the *ab*-plane. The value of the cobalt-cobalt distance is 7.770(2) Å and 9.041(2) Å (Figure 4b). The hydrogen bonded layers are further held together by means of the π···π interactions between two adjacent triazole rings with the center-to-center separation: 3.990(1) Å, which resulting in a 3D structure (Figure 4c).

(a)

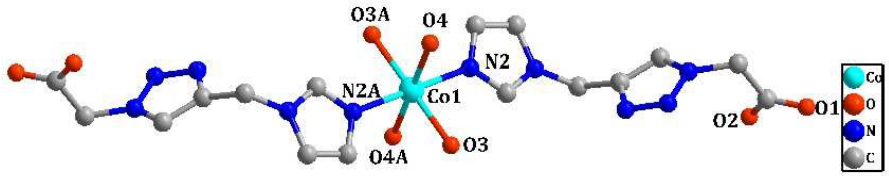

(b)

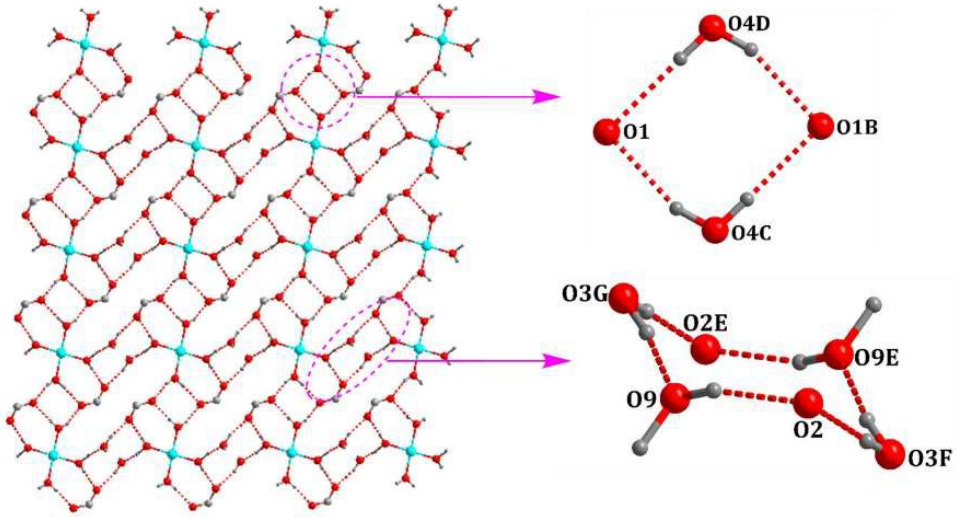

(c)

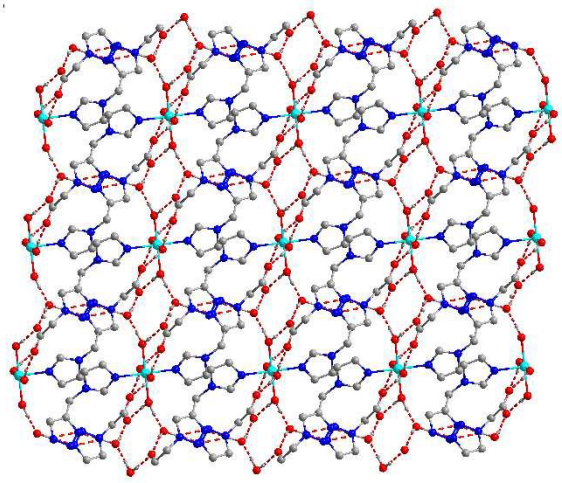

Figure 4. (a) The surrounding coordination environment of complex **6** (symmetry codes for A:-x+1,-y,-z+2). (b) Alternate connection of $R_2^4(8)$ and $R_4^6(12)$ rings in the 2-D supramolecular layer (symmetry codes for B: -x, 2-y, -z; for C: -x, 1-y, 1-z; for D: x, 1+y, z-1; E: 1-x, 1-y, -z; F: 1-x, 1-y, 1-z; G: x, y, -1+z). (c) 3-D supramolecular network constructed via O-H···O and N-H···O interactions.

The effect of various reaction variables on building the architectures of complexes 2 (or **3**) and **6** (or **7**)

As we all know, the prediction of complex structures is still subjective and cannot be generalized because the final structures are frequently modulated by various factors. To have a systematic and comprehensive investigation of various subtle influence factors on the complex structures, herein, we present two Co(II) [and two Mn(II)] coordination complexes **2** (**3**) and **6** (**7**), in which **2** (**3**) displays 3D framwork and **6** (**7**) presents mononuclear structure, respectively. Interestingly, the analogous results could be observed between **3** and **7**, **2** and **6** are accordingly selected to be discussed in detail. The following observations were detailed in Table 3 and supported by PXRD patterns (Figure 5 and Figure S1).

(i) When the mole ratio of Himta/$CoCl_2 \cdot 6H_2O$ was 2:1, reaction temperature was controlled in 105°C and solvent composition of H_2O/CH_3OH was 1 mL/2 mL, polymer **2** was obtained (Table 3). However, when the ratio of L/M was less than 2:1

and kept the other conditions unchanged, complex **6** was prepared. From the subtle changes, we speculate that it might be due to the difference of trace amount of water from the metal salt. In **6**, the water molecules as terminal ligands participate in the coordination. With the increasing amount of crystallization water in the metal salts, the coordination of water molecule with the metal becomes more favorable.

(ii) Based on the above thoughts, the amount of water may be one of the factors that affect the structures of complex. Then we still kept the mole ratio of L/M was 2:1 (Table 3), reaction temperature was 105°C, but increased the content of water in solvents system, in which H_2O/CH_3OH were 3mL/4mL, 3mL/1mL, 5mL/1mL, 6mL/0mL. As expected, all of the reaction conditions afforded complex **6**. From the coordination equilibrium point of view, there are strong competition between the water molecule and the carboxylate group of imta. The increasing H_2O content in the solvent has an important impact on the Co(II) coordination environment established during the solvothermal process, in which the water molecules acting as terminal ligands.[29] The above results implied that the expected structural motifs can be achieved by changes in stoichiometry.

(iii) To determine whether or not temperature influences the two complex structures (Table 3), the parallel experiments were carried out by using $CoCl_2 \cdot 6H_2O$ with Himta in H_2O/CH_3OH (1 mL/2 mL) solvent system at a L/M ratio of 2:1. By control of the temperature at 95, 105, 120, 130, 150, 160°C respectively, polymer **2** was obtained at 95, 105 and 120°C, while complex **6** were obtained at 130~160°C. It is found that the polymer **2** with 3-D structure preferred to form around 105°C. The above results apparently indicate that the temperature can dramatically affect the final complex structures.

That the same reactions conducted at different temperature afforded different structure forms, prompted us to take a systematic approach to address what influence temperature and water content might have upon the structures of **2** and **6**. Hence, we repeated experiment (i) and just adjusted temperature to 95°C, while the other experimental conditions were kept constant. The final products and the variable conditions of L/M, solvent systems are summarized in Table 3. It is evident that the

L/M ratio plays a very limited role in determining the final products. Under the condition of 105°C, the clear exception occurs at the boundary between the **2** and **6**, where only the highest L/M ratio of 2:1 were observed to favor polymer **2**, while lower L/M ratios favored complex **6**. However, polymer **2** were obtained under the conditions of all given L/M ratios at 95°C. This indicates that temperature effect seem to be more important than the trace amount of crystallization water effect in these systems. The role of temperature in controlling complex architectures can be rationalized as higher temperatures would naturally be expected to afford more thermodynamically stable crystal forms, which results in complex **6**. While from the coordination equilibrium point of view, we are still inclined to think that complex **6** can be obtained with the increase of the amount of water. So we repeated experiment (ii) and only changed temperature to 95°C. As was expected, complex **6** is obtained under the given conditions. This proves that water content in solvent system is more important on self-assembly of the supramolecular entity. The result is consistent with so-called "concentration effect" of previous reports,[12,13] in which the concentration also has an effect on complex structures. We also attempted to crystallize at other mixture solvents and other ratios of H_2O/CH_3OH, but always failed to form any crystals suitable for X-ray determination. Although the influences of temperature and water content on structures are only observed in a certain range, the results described herein provide an indication that simple but efficient ways to control complex structures are at hand.

(iv) Finally, in order to evaluate the influence of counteranions on complex structures, $Co(NO_3)_2{\cdot}6H_2O$, $Co(Ac)_2{\cdot}4H_2O$ and $CoSO_4{\cdot}7H_2O$ were used instead of $CoCl_2{\cdot}6H_2O$ to react with Himta. Experimental conditions are described in detail in Table 3. The results indicated that there is no great influence of Cl^- and NO_3^- on the structure of the polymer **2**, but the $Co(Ac)_2{\cdot}4H_2O$ can lead to a structure of complex **6**. The same results were obtained through the repeated experiments. It is well known that anion effects are important because they can adjust the properties of the complexes and affect their structures either by coordinating directly to the metal centers or by acting as templates that reorganize the organic building blocks.[30] It

proved that anions play subtle roles in the supramolecular assemblies. We also attempted to crystallize with $CoSO_4 \cdot 7H_2O$ and Himta, but always failed to form any crystals suitable for X-ray determination.

It should be pointed out that similar phenomena also occur between **3** and **7**. The bulk purity of **2** (and **6**) or **3** (and **7**) was confirmed by comparing its experimental powder X-ray diffraction (PXRD) pattern to that simulated based on the single crystal structure (Figure 5 and Figure S1).

Table 3. *Summary of the products isolated at different condition*

	Himta/$CoCl_2 \cdot 6H_2O$(mmol)	H_2O/CH_3OH(mL)	T/°C	Complex
(i). Different ratio of L/M	0.04/0.02	1/2	105 (95)	**2** (**2**)
	0.04/0.03	1/2	105 (95)	**6** (**2**)
	0.03/0.03	1/2	105 (95)	**6** (**2**)
	0.04/0.04	1/2	105 (95)	**6** (**2**)
(ii). Different ratio of H_2O/CH_3OH	0.04/0.02	3/4	105 (95)	**6** (**6**)
	0.04/0.02	3/1	105 (95)	**6** (**6**)
	0.04/0.02	5/1	105 (95)	**6** (**6**)
	0.04/0.02	6/0	105 (95)	**6** (**6**)
(iii). Different temperature	0.04/0.02	1/2	95	**2**
	0.04/0.02	1/2	105	**2**
	0.04/0.02	1/2	120	**2**
	0.04/0.02	1/2	130	**6**
	0.04/0.02	1/2	150	**6**
	0.04/0.02	1/2	160	**6**
(iv). Different anion	L/M 0.04/0.02(mmol)	H_2O/CH_3OH(mL)	T/°C	
	$Co(NO_3)_2 \cdot 6H_2O$	1/2	105	**2**
	$CoSO_4 \cdot 7H_2O$	1/2	105	**-**
	$Co(Ac)_2 \cdot 4H_2O$	1/2	105	**6**

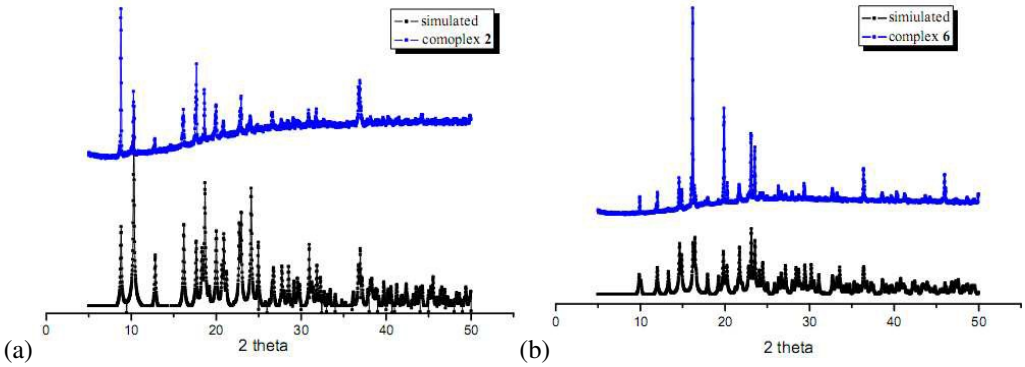

Figure 5. Powder X-ray diffraction (PXRD) patterns of **2** and **6**: (a) simulated PXRD pattern from the single crystal structure of **2** (black), observed PXRD pattern of **2** at room temperature (blue). (2) simulated PXRD pattern from the single crystal of **6** (blue), observed PXRD pattern of **6** at room temperature (black).

Luminescent Properties.

The fluorescence properties of Himta ligand and complexes **2~9** have been studied in solid state at room temperature and the results were shown in Figure 6. The free ligand exhibits a broad emission peak centered at 446 nm (λ_{ex}=370 nm) for Himta, which may be assigned to the $\pi\rightarrow\pi^*$ transitions. Almost no luminescent emission for complexes **2** and **6** can be observed, which is obviously due to fluorescence quenching effects of Co(II).[31] It should be noted that that complex **3** shows no luminescent emission, but complex **7** shows an emission at 424 nm (λ_{ex}=367 nm), which may be assigned to the ($\pi\rightarrow\pi^*$) intraligand fluorescence and ligand-to-metal charge transfer.[32] For **4**, the emission bands around 376 nm (λ_{ex}=310 nm) can be attributed to the ($\pi\rightarrow\pi^*$) intraligand fluorescence. The blue shift of emission bands for **4** may be due to the distortion of ligands caused by the coordination interactions between the metals and the ligands.[33,32c] Polymer **5** exhibits an intense emission at 458 nm (λ_{ex}=308 nm), exhibiting a slight red-shift compared to that of free Himta. Similar phenomenon have been observed for other s^2-metal complexes, which can be assigned to a metal-centered transition involving the s and p metal orbital.[34] The complex **8** shows very weak emissions, which may probably be quenched by the Ni(II). Interestingly, complex **9** exhibits enhanced emission with peak maxima at 424 nm (λ_{ex}=362 nm). The increase intensity may be ascribed to the increase conformational rigidity due to the ligand coordination to Zn(II) resulting in an enhaced intraligand ($\pi\rightarrow\pi^*$) fluorescent emission.[35]

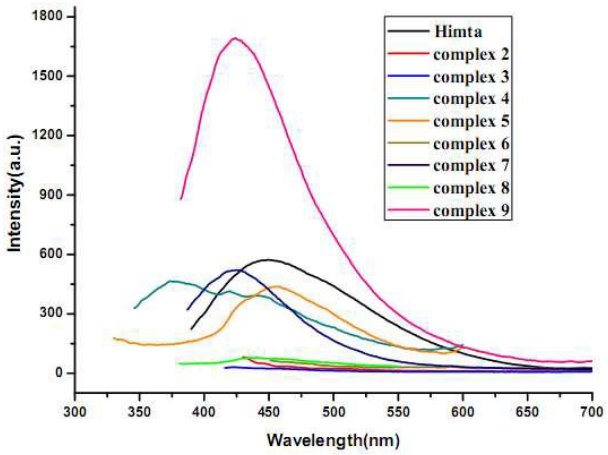

Figure 6. The emission spectra of complexes **2~9** and Himta in the solid state at room temperature.

Conclusion

In summary, nine new complexes with different structures and topologies under solvothermal conditions were obtained with an N-heterocyclic carboxylic acid Himta. A systematic and comprehensive investigation of temperature, solvent, M/L ratios and anion on complex architectures have been carried out. Our results elucidate the roles of M/L ratio, H_2O/CH_3OH ratio, temperature, and concentration in determining specific structure forms. From the coordination equilibrium point of view, the increasing H_2O content in solvent systems, as terminal ligands, has an important impact on complex structures. The temperature can dramatically affect the final complex structures, in which the higher temperatures can afford the more thermodynamically stable crystal forms. The anions also play the subtle roles in the supramolecular assemblie by acting as templates. This work may help unravel the mechanism for the roles that synthesis parameters play in the formation of complex structures and provides insight into the discovery of new compounds. The luminescence mechanisms of complexes **2~9** were also discussed in details. Complex **9** show strong fluorescence emissions, signifying that the complex may be good candidate for optical materials.

Acknowledgment. This work was financially supported by the National Natural Science

Foundation (Nos 21273205, 21401168, J1210060, U1204203 and 21543011).

Supporting Information Available: X-ray crystallographic data, selected bond lengths and bond angles, powder X-ray patterns. This information is available free of charge via the Internet at http://pubs.acs.org/.

References

(1) H. J. Li, B. Zhao, R. Ding, Y. Y. Jia, H. W. Hou, Y. T. Fan, *Cryst. Growth Des*., 2012, 12, 4170-4179. (b) B. H. Ye, M. L. Tong, X. M. *Chen, Coord. Chem. Rev*., 2005, 249, 545-565. (c) K. Suzuki, M. Kawano, M. Fujita, *Angew. Chem., Int. Ed*., 2007, 46, 2819-2822. (g) H. N. Miras, I. Chakraborty, R. G. Raptis, *Chem. Commun*., 2010, 46, 2569-2571. (e) F. Y. Lian, F. L. Jiang, D. Q. Yuan, J. T. Chen, M. Y. Wu, M. C. Hong, *CrystEngComm*, 2008, 10, 905-914.

(2) (a) J. S. Mendy, M. A. Saeed, F. R. Fronczek, D. R. Powell, M. A. Hossain, *Inorg. Chem*., **2010**, 49, 7223-7255. (b) M. Meilikhov, K. Yusenko, A. Torrisi, B. Jee, C. Mellot-Draznieks, A. Pöppl, R. A. Fischer, *Angew. Chem., Int. Ed.,* **2010**, 49, 6212-6215. (c) J. P. Li, L. K. Li, H. W. Hou, Y. T. Fan, *Cryst. Growth Des.*, **2009**, 9, 4504-4513. (d) Z. Z. Lu, R. Zhang, Y. Z. Li, Z. J. Guo, H. G. Zheng, *J. Am. Chem. Soc*., **2011**, 133, 4172-4174. (f) Z. J. Zhang, W. Y Gao, L. Wojtas, S. Q. Ma, M. Eddaoudi, M. J. Zaworotko, *Angew. Chem., Int. Ed*., **2012**, 51, 9330-9334. (g) D. Liu, J. P. Lang, B. F. Abrahams, *J. Am. Chem. Soc*., **2011**, 133(29), 11042-11045.

(3) (a) A. K. Cheetham, G. Férey, T. Loiseau, *Angew. Chem., Int. Ed*., **1999**, 38, 3268-3292. (b) A. K. Cheetham, C. N. R. Rao, R. K. Feller, *Chem. Commun*., **2006**, 4780-4795. (c)S. F. L. Mertens, C. Vollmer, A. Held, M. H. Aguirre, M. Walter, C. Janiak, T. Wandlowski, *Angew. Chem., Int. Ed*., **2011**, 50, 9735-9738.(d) J. P. Li, L. Liu, T. T. Hou, H. Sun, Y. Y. Zhu, S. M. Wang, J. H. Wu, H. Xu; Y. X. Guo, B. X. Ye, H. W. Hou, Y. T. Fan, J. B. Chang, *J. Coord. Chem.*, **2012**, 65, 3684-3698. (e) H. Y. Zhao, Z. Jin, H. M. Su, J. L. Zhang, X. D. Yao, H. J. Zhao, G. S. Zhu, *Chem. Commun.*, **2013**, 49, 2780-2782. (f) S. Horike, M. Dincă, K. Tamaki, J. R. Long, *J. Am. Chem. Soc*., **2008**, 130, 5854-5855. (g) S. K. Henninger, H. A. Habib, C, Janiak. **2009**, *J. Am. Chem. Soc*., 131, 2776-2777.

(4) (a) Y. Zhang, J. Yang, Y. Yang, J. Guo, J. F. Ma, *Cryst. Growth Des*., **2012**, 12, 4060-4071. (b)

J. P. Li, L. K. Li, H. W. Hou, Y. T. Fan, *J. Organomet. Chem.*, **2009**, 694, 1359-1368.

(5) (a) B. L. Chen, F. R. Fronczek, A. W. Maverick, *Chem. Commun.*, **2003**, 2166-2167. (b) X. H. Bu, Y. B. Xie, J. R. Li, R. H. Zhang, *Inorg. Chem*., **2003**, 42, 7422-7430.

(6) (a) Q. Zhang, J. Y. Zhang, Q. Y. Yu, M. Pan, C. Y. Su, *Cryst. Growth Des.*, **2010**. 10. 4076-4084. (b) J. Y. Lu, *Coord. Chem. Rev.*, **2003**, 246, 327-347.

(7) (a) J. A. K. Howard, H. A. Sparkes. *CrystEngComm*, **2008**, 10, 502-506. (b) Y. L. Gai, F. L. Jiang, K. C. Xiong, L. Chen, D. Q. Yuan, L. J. Zhang, K. Zhou, M. C. Hong, *Cryst. Growth Des.*, **2012**, 12, 2079-2088.

(8) (a) K. A. Hirsch, S. R. Wilson, J. S. Moore, *Inorg. Chem*., **1997**, 36, 2960-2968. (b) Y. R. Liu, J. P. Li, H. W. Hou, Y. T. Fan, *J. Organomet. Chem.*, **2009**, 694, 2875-2882.

(9) (a) P. Cui, L. J. Ren, Z. Chen, H. C. Hu, B. Zhao, W. Shi, P. Cheng, *Inorg. Chem*., **2012**, 51, 2303-2310. (b) Y. B. Dong, Y. Y. Jiang, J. Li, J. P. Ma, F. L. Liu, B. Tang, R. Q. Huang, S. R. Batten, *J. Am. Chem. Soc*., **2007**, 129, 4520-4521. (c) J. Y. Lee, S. Y. Lee, W. Sim, K. M. Park, J. Kim, S. S. Lee, *J. Am. Chem. Soc*., **2008**, 130, 6902-6903 (d) P. Kanoo, K. L. Gurunatha, T. K. Maji, *Cryst. Growth Des*., **2009**, 9, 4147-4156. (e) J. J. Wu, W. Xue, M. L. Cao, Z. P. Qiao, B. H. Ye, *CrystEngComm*, **2011**, 13, 5495-5501.

(10) (a) P. P. Cui, J. L. Wu, X. L. Zhao, D. Sun, L. L. Zhang, J. Guo, D. F. Sun, *Cryst. Growth Des.,* **2011**, 11, 5182-5187. (b) B. L. Chen, F. R. Fronczek, A. W. Maverick, *Chem. Commun.*, **2003**, 2166-2167. (c) E. Tynan, P. Jensen, P. E. Kruger, A. C. Lees, *Chem. Commun.*, **2004**, 776-777. (d) K. I. Nättinen, K. Rissanen. *Inorg. Chem.,* **2003**, 42, 5126-5134. (e) Q. Gao, Y. B. Xie, J. R. Li, D. Q. Yuan, A. A. Yakovenko, J. H. Sun, H. C. Zhou, *Cryst. Growth Des*., **2012**, 12, 281-288.

(11) (a) L. Wang, Z. H. Yan, Z. Y. Xiao, D. Guo, W. Q. Wang, Y. Yang, *CrystEngComm*, **2013**, 15, 5552-5560. (b) R. H. Wang, M. C. Hong, W. P. Su, Y. C. Liang, R. Cao, Y. J. Zhao, J. B. Weng, *Inorg. Chim. Acta*, **2001**, 323, 139-146. (c) R. P. Feazell, C. E. Carson, K. K. Klausmeyer. *Eur. J. Inorg. Chem*., **2005**, 3287-3297. (d) S. Q. Zang, M. M. Dong, Y. J. Fan, H. W. Hou, T. C. W. Mak. *Cryst. Growth Des.,* **2012**, 12, 1239-1246.

(12) J. J. Zhang, L. Wojtas, R. W. Larsen, M. Eddaoudi, M. J. Zaworotko, *J. Am. Chem. Soc.*, **2009**, 131, 17040-17041.

(13) P. M. Forster, N. Stock, A. K. Cheetham, *Angew. Chem., Int. Ed.*, **2005**, 44, 7608-7611.

(14) J. Warnan, Y. Pellegrin, E. Blart, F. Odobel, *Chem. Comm*., **2012**, 48, 675-677.

(15) G. M. Sheldrick, *Acta. Cryst . A.* **2008**, 64, 112-122.

(16) C. Janiak, *J. Chem. Soc., Dalton Trans.,* **2000**, 3885-3896

(17) N. L. Rosi, J. Kim, M. Eddaoudi, B. L. Chen, M. O'Keeffe, O. M. Yaghi, *J. Am. Chem. Soc.,* **2005**, 127, 1504-1518.

(18) (a) Blatov, V. A. IUCr CompComm Newsletter 2006, 7, 4. (b) Blatov, V. A. TOPOS, A Multipurpose Crystallochemical Analysis with the Program Package; Samara State University: Samara, Russia, 2009.

(19) L. Shimoni-Livny, J. P. Glusker, C. W. Bock, *Inorg. Chem*., **1998**, 37, 1853-1867.

(20) H. Sun, Y. N. Zhang, X. Q. Si, J. P. Li, X. L. Gao, J. B. Chang, Y. R. Liu, Y. X. Guo, H. W. Hou, Y. T. Fan, *Synth. React. Inorg. Met-org. Chem.* **2013**, 43, 739-745.

(21) X. Y. Zhang, Y. H. Zhang, S. Z. Liu, H. Xu, J. P. Li, H. W. Hou, *Inorg. Chem. Commun.*, **2014**, 46, 289-294.

(22) L. Shimoni-Livny, J. P. Glusker, C. W. Bock, *Inorg. Chem.*, **1998**, 37, 1853-1867.

(23) S. J. Li, W. D. Song, D. L. Miao, D. Y. Ma, *Chinese J. Struct. Chem.*, **2011**, 7, 1049-1053.

(24) Bruker (**2007**). *SMART and SAINT*. Bruker AXS Inc., Madison, Wisconsin, USA.

(25) (a) G. M. Sheldrick, *SHELXS-97*, *Program for X-ray Crystal Structure Solution*, Göttingen University, Germany **1997**. (b) G. M. Sheldrick, *SHELXL-97*, *Program for X-ray Crystal Structure Refinement*, Göttingen University, Germany **1997**.

(26) X. M. Chen, J. W. Cai, *Single-Crystal Structural Analysis Principles and Practices,* the Science Press, Beijing, **2003**.

(27) J. H. Wang, G. M. Tang, Y. T. Wang, T. X. Qin, S. W. Ng, *CrystEngComm,* **2014**, 16, 2660-2683.

(28) A. Chakraborty, P. Bag, J. Goura, A. K. Bar, J. P. Sutter, V. Chandrasekhar, *Cryst. Growth Des.*, **2015**, 15, 848-857.

(29) M. Mazaj, T. B. Čelič, G. Mali, M. Rangus, V. Kaučič, N. Z. Logar, *Cryst. Growth Des.*, **2013**, 13, 3825-3834.

(30) J. P. Li, X. F. Li, H. J. Lü, Y. Y. Zhu, H. Sun, Y. X. Guo, Z. F. Yue, J. A. Zhao, M. S. Tang, H. W. Hou, Y. T. Fan, J. B. Chang, *Inorg. Chim. Acta*, **2012**, 384, 163-169.

(31) Y. Zhang, X. B. Luo, Z. L. Yang, G. Li, *CrystEngComm*, **2012**, 14, 7382-7397.

(32) (a) Y. Zhuang, X. H. Yin, P. F. Li, F. L. Hu, S. S. Zhang, J Chem Crystallogr, **2012**, 42, 18-23. (b) X. J. Huang, Y. N. Xia, H. R. Zhang, Z. Z. Yan, Y. Tang, X. J. Yang, B. Wu, *Inorg. Chem. Commun.*, **2008**, 11, 450-453. (c) F. L. Liu, L. L. Zhang, R. M. Wang, J. Sun, J. Yang, Z. Chen, X. P. Wang, D. F. Sun, *CrystEngComm*, **2014**, 16, 2917-2928.

(33) C. S. Liu, J. J. Wang, Z. Chang, L. F. Yan, X. H. Bu, *CrystEngComm*, **2010**, 12, 1833-1841.

(34) G. P. Yang, L. Hou, Y. Y. Wang, Y. N. Zhang, Q. Z. Shi, S. R. Batten, *Cryst. Growth Des.*, **2011**, 11, 936-940.

(35) C. J. Wang, T. Wang, L. Li, B. B. Guo, Y. Zhang, Z. F. Xiong, G. Li, *Dalton Transactions.* **2012**, 00, 1-11.

Table 1. Crystal data and structure refinement for complexes **1~5**

Complex	**1**	**2**	**3**	**4**	**5**
Formula	$C_{32}H_{42}Cu_2N_{20}O_{13}$	$C_{16}H_{16}CoN_{10}O_4$	$C_{16}H_{16}MnN_{10}O_4$	$C_{16}H_{16}CdN_{10}O_4$	$C_{16}H_{16}N_{10}O_4Pb$
Fw	1041.94	471.32	467.33	524.79	619.59
Temp(K)	293(2)	293(2)	288(2)	293(2)	293(2)
Wavelength(Å)	0.71073	0.71073	0.71073	0.71073	0.71073
Crystal syst	Monoclinic	Monoclinic	Monoclinic	Monoclinic	Orthorhombic
Space group	*I2/a*	*P2(1)/c*	*P2(1)/c*	*P2(1)/c*	*Pccn*
a(Å)	8.2134(16)	4.8427(10)	4.9140(10)	4.9534(10)	10.487(2)
b(Å)	16.974(3)	9.4938(19)	9.3923(19)	9.1796(18)	23.350(5)
c(Å)	19.396(6)	20.097(4)	20.417(4)	20.865(4)	8.3772(17)
α(deg)	90	90	90	90	90
β(deg)	101.13(3)	92.37(3)	92.66(3)	93.90(3)	90
γ(deg)	90	90	90	90	90
V(Å^3)	2653.2(11)	923.2(3)	941.3(3)	946.5(3)	2051.3(7)
Z	2	2	2	2	4
D_c(g·cm^{-3})	1.304	1.696	1.649	1.841	2.006
F(000)	1072	482	478	524	1184
θ range for data collection(deg)	2.14~24.98	2.03~24.99	2.00~27.84	2.42~25.00	2.13~27.88
Reflections collected/unique	8801 / 2329	6033 / 1628	7614 / 2219	6072 / 1656	7875 / 2427
Data/ restraints / params	2329/ 6 / 175	1628 / 0 / 142	2219 / 0 / 142	1656 / 0 / 142	2427 / 0 / 141
Goodness-of-fit on F^2	0.986	0.960	1.125	1.013	1.151
FinalR1[a], wR2[b]	0.0788, 0.2186	0.0562, 0.1620	0.0577, 0.1036	0.0364, 0.0694	0.0508, 0.0721

[a] $R1 = ||F_o| - |F_c|| / |F_o|$. [b] $wR2 = [w(|F_o^2| - |F_c^2|)^2 / w|F_o^2|^2]^{1/2}$. $w = 1/[\sigma^2(F_o)^2 + 0.0297P^2 + 27.5680P]$, where $P = (F_o^2 + 2F_c^2)/3$.

Table 2. Crystal data and structure refinement for complexes **6~9**

Complex	**6**	**7**	**8**	**9**
Formula	$C_{16}H_{28}CoN_{10}O_{10}$	$C_{16}H_{28}MnN_{10}O_{10}$	$C_{16}H_{28}N_{10}NiO_{10}$	$C_{16}H_{28}N_{10}O_{10}Zn$
Fw	579.41	575.42	579.17	585.87
Temp(K)	293(2)	293(2)	293(2)	293(2)
Wavelength(Å)	0.71073	0.71073	0.71073	0.71073
Crystal syst	Triclinic	Triclinic	Triclinic	Triclinic
Space group	*P-1*	*P-1*	*P-1*	*P-1*
a(Å)	7.7702(16)	7.8231(16)	7.7318(15)	7.7881(16)
b(Å)	9.0412(18)	9.0961(18)	8.9961(18)	9.0380(18)
c(Å)	9.2461(18)	9.2962(19)	9.1815(18)	9.1899(18)
α(deg)	94.47(3)	94.66(3)	94.40(3)	94.47(3)
β(deg)	107.46(3)	107.53(3)	107.22(3)	107.49(3)
γ(deg)	95.08(3)	95.54(3)	95.01(3)	95.27(3)
V(Å^3)	1781.2(6)	3514.2(11)	1360.5(5)	1921.1(7)
Z	1	1	1	1
D_c(g·cm^{-3})	1.568	1.532	1.592	1.593
F(000)	301	287	302	304
θ range for data collection(deg)	2.28~25.00	2.26~25.00	2.29~27.87	2.28~27.86
Reflections collected/unique	5983 / 2153	5509 / 2190	6203 / 2849	6755 / 2874
Data/ restraints / params	2153 / 0 / 201	2190/0/ 169	2849 / 12 / 192	2874/3/193
Goodness-of-fit on F^2	1.068	1.121	1.034	1.037
Final$R1$[a], w$R2$[b]	0.0370,0.0804	0.0491, 0.1419	0.0486, 0.1093	0.0410, 0.0707

[a] $R1 = \sum||F_o| - |F_c|| / \sum|F_o|$. [b] w$R2 = [\sum w(|F_o^2| - |F_c^2|)^2 / \sum w|F_o^2|^2]^{1/2}$. $w = 1/[\sigma^2(F_o)^2 + 0.0297P^2 + 27.5680P]$, where $P = (F_o^2 + 2F_c^2)/3$.

Illustration

Roles of Temperature, Solvent, M/L ratios and Anion in Preparing the Complexes Containing Himta Ligand

Tiantian Yu, Shimin Wang, Xuemin Li, Xiaoli Gao, Chunlin Zhou, Jiajia Cheng, Baojun Li, Jinpeng Li*, Junbiao Chang, Hongwei Hou, Zhongyi Liu*

A graphical contents entry

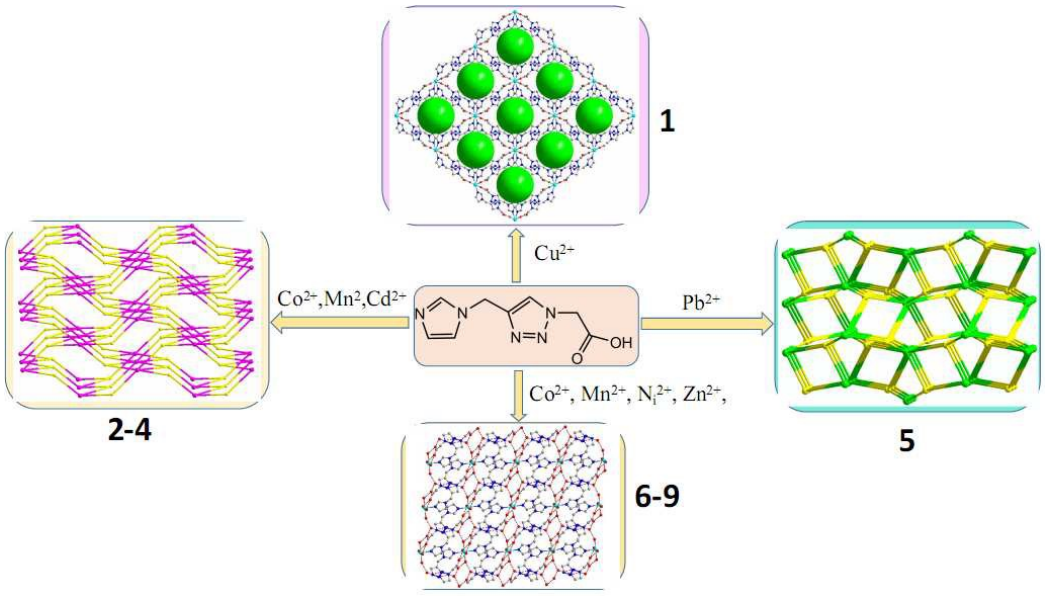

Nine new complexes based Himta ligand were hydrothermally synthesized and structurally characterized. A systematic and comprehensive investigation of four influence factors on some complex architectures were carried out.